Proc. Natl. Acad. Sci. USA
Vol. 90, pp. 5909–5913, July 1993
Biochemistry

Hydroxyl radical footprint analysis of human immunodeficiency virus reverse transcriptase–template•primer complexes

(AIDS/RNase H mutants/arrested polymerization)

WILLI METZGER*, THOMAS HERMANN*, OCTAVIAN SCHATZ†, STUART F. J. LE GRICE‡, AND HERMANN HEUMANN*§

*Max Planck Institute of Biochemistry, D-8033 Martinsreid, Germany; †Vienna International Research Cooperation Center, Laboratory of Somatic Gene Therapy, Brunnerstrasse 59, A-1235 Vienna, Austria; and ‡Division of Infectious Diseases, Case Western Reserve University School of Medicine, Cleveland, OH 44106

Communicated by Frederick C. Robbins, March 19, 1993 (received for review December 30, 1992)

ABSTRACT **Human immunodeficiency virus type 1 reverse transcriptase protects sugar moieties of a model template•primer DNA in a region from positions +3 to −15 from hydroxyl radical attack. A protected region of equivalent size migrates in concert with the translocating enzyme, as shown by hydroxyl radical footprints of replication complexes after primer extension by 4, 10, and 19 nt. The pattern of these footprints suggests that the DNA template•primer is in the A conformation when complexed with reverse transcriptase. Enhanced accessibility of the DNA template strand around position −15 to hydroxyl radicals indicates a conformational change in the template induced by the C-terminal RNase H-containing domain of p66 reverse transcriptase.**

Inhibition of human immunodeficiency virus reverse transcriptase (HIV RT) remains one of the most significant approaches in the fight against acquired immunodeficiency syndrome (AIDS). Combination therapy, using various RT inhibitors, has been discussed as a possible means of enhancing drug tolerance and reducing problems of drug resistance (1–4). Information regarding the structure of the retroviral polymerase would be an obvious advantage when attempting to design inhibitors with improved efficacy. A recent series of publications dealing with the structure of HIV-1 RT with enhanced resolution serves to emphasize this view. A neutron solution scattering study (5) has provided information about the spatial arrangement of the RT domains, and a crystal structure analysis of an RT–antibody complex at 0.35-nm resolution (6) has revealed the arrangement of the active sites within RT. Although recent publication of a structure model of Kohlstaedt *et al.* (7) at 0.3-nm resolution is sufficiently detailed to be considered useful for designing anti-RT drugs, there is little information about the structure of RT in complex with its RNA and DNA templates. The x-ray structure analysis of Arnold *et al.* (6) included template DNA, which was allowed to diffuse into the RT crystal, giving an approximate position of the template. However, the accuracy of the data was insufficient to determine whether the template DNA was in the A or B conformation. Kohlstaedt *et al.* (7) placed a template in the A conformation into the structure of isolated RT and presented a rather detailed picture of the complex. However, no study to date has revealed information on HIV RT during polymerization events, to our knowledge.

As a complementary approach to crystallographic analyses, we have used hydroxyl radical footprinting (8) to provide experimental evidence for contacts between p66/p51 HIV-1 RT (wild-type and RNase H-deficient forms) and the sugar moieties of a synthetic duplex DNA during primer elongation. Hydroxyl radical footprinting can be considered a biochemical approach providing high-resolution structural information (8) about the interface between DNA and a DNA-binding protein. Iron–EDTA-generated hydroxyl radicals most likely attack nucleotide sugars at the C1 and C4 positions, leading to excision of a base. A hydroxyl radical footprint reflects reduced accessibility of the DNA sugar moieties due to protection by a bound protein. The resolution of this method is determined by the distance of neighboring bases in DNA, which is in the range of 0.3 nm. Examples of DNA binding proteins that have been studied by this technique include nuclear factor 1 (9), bacteriophage λ repressor (10), restriction endonuclease *Eco*RI (11), and *Escherichia coli* RNA polymerase (12).

We have used hydroxyl radicals to determine contact points between a duplex DNA template•primer on which RT-catalyzed DNA synthesis was "arrested" at several positions along the template by incorporation of a chain-terminating dideoxynucleoside triphosphate (ddNTP). Such complexes would be a reasonable approximation of DNA-dependent DNA polymerase activity catalyzed by the retroviral polymerase during (+)- or second-strand synthesis (13). This approach has allowed us to study interactions with both the template and primer strands and to make predictions on the structure of RT-bound template•primer during polymerization.

MATERIALS AND METHODS

Preparation of HIV-1 RT. Heterodimer (p66/p51) HIV-1 RT was prepared from the *E. coli* M15::pDMI.1::pRT6H-PR (14) and the RNase H-deficient derivative from strain M15::pDMI.1::p6HRT$^{E\rightarrow Q}$-PR (15, 16). Both enzymes were purified by a combination of metal chelate (Ni^{2+}-nitrilotriacetic acid-Sepharose) and ion-exchange chromatography (DEAE-Sepharose and S-Sepharose) as described (14, 17). Enzyme preparations were judged to be at least 90% homogeneous and free of contaminating nucleases. Purified enzymes were stored at −20°C in a 50% (vol/vol) glycerol-containing buffer.

Synthesis and Purification of Oligodeoxynucleotides. Oligodeoxynucleotides representing the template and primer strands depicted in Fig. 1*a* were prepared from phosphoramidites on an Applied Biosystems chemical synthesizer. Final purification was achieved by electrophoresis through denaturing 12% or 20% polyacrylamide gels containing 7 M urea, 90 mM Tris borate, and 0.2 mM EDTA (pH 8.3). DNA of the correct length was visualized either by UV-shadowing (254 nm) or, after end-labeling with [γ-^{32}P]ATP, by autora-

The publication costs of this article were defrayed in part by page charge payment. This article must therefore be hereby marked "*advertisement*" in accordance with 18 U.S.C. §1734 solely to indicate this fact.

Abbreviations: HIV, human immunodeficiency virus; RT, reverse transcriptase; ddNTP, dideoxynucleoside triphosphate.

§To whom reprint requests should be addressed.

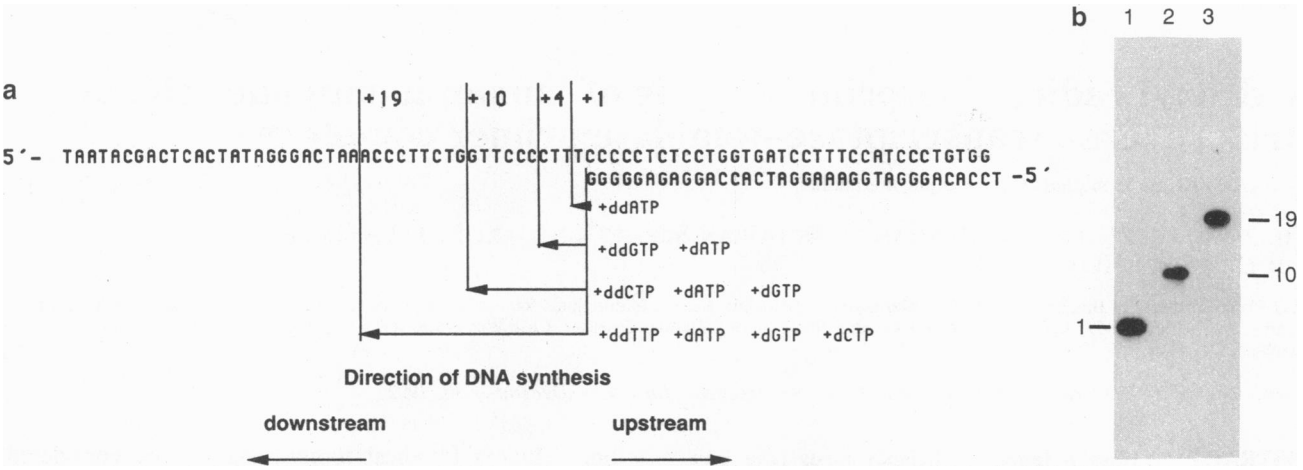

FIG. 1. (*a*) Sequence of synthetic template·primer used for arresting HIV-1 RT-catalyzed DNA synthesis at specific base positions. Indicated under the DNA sequence of the template·primer are the dNTP/ddNTP combinations required to produce arrested polymerization complexes containing primer DNA extended by 1, 4, 10, or 19 nt. (*b*) Analysis of arrested polymerization complexes by high-resolution gel electrophoresis. The 5′ ^{32}P-end-labeled primer DNA from polymerase reaction mixtures, extended by 1, 10, and 19 bases (lanes 1–3, respectively), was fractionated through a 20% polyacrylamide gel containing 8 M urea. Note the absence of prematurely aborted complexes in both the +10 and +19 complexes (lanes 2 and 3, respectively).

diography. Bands were excised and eluted by shaking overnight in sterile 0.3 M sodium acetate (pH 7.5). DNA in the eluate was precipitated by addition of 3 vol of 95% ethanol, collected by centrifugation, washed with 70% ethanol, dried, and resuspended in 10 mM Tris·HCl, pH 7.0/1 mM EDTA.

Labeling of Oligodeoxynucleotides. The 5′-end-labeling of the 78-mer DNA template and 35-mer primer was accomplished with [γ-^{32}P]ATP (Amersham) and T4 polynucleotide kinase by the procedures of Maniatis *et al.* (18). The 3′-end-labeling of the template was achieved using the Klenow fragment of DNA polymerase I and [α-^{32}P]dATP.

Formation of RT–DNA Complexes and Elongation of the Primer. Approximately 0.5 μg of annealed template·primer was incubated with stoichiometric amounts of wild-type or mutant enzyme in RT reaction buffer (60 mM NaCl/6 mM $MgCl_2$/5 mM dithiothreitol/40 mM Tris·HCl, pH 8.0) for 10 min at 37°C. The appropriate dNTP/ddNTP mixture that allowed a defined stop (see Fig. 1*a*) was then added, after which the elongation reaction mixture was incubated at 37°C for 20 min. The final total dNTP concentration in an elongation mixture was 50 μM, whereas the chain-terminating ddNTP was supplemented at 500 μM.

Treatment of Polymerization Complexes with Hydroxyl Radicals. Hydroxyl radical footprinting was essentially performed as described in Tullius and Dombroski (8) and Schickor *et al.* (12). After hydroxyl radical treatment, samples were precipitated with ethanol, dried, dissolved in 50% (vol/vol) formamide, and analyzed by high-voltage electrophoresis on 12% polyacrylamide gels containing 8 M urea. For autoradiography, the gel was exposed to Trimax x-ray film.

Molecular Modeling. Molecular modeling of template·primer in either A or B conformation was accomplished with an Evans and Sutherland PS390 workstation using SYBYL software provided by Tripos Associates (St. Louis).

RESULTS

Preparation of Complexes Arrested in Specific Registers. Application of footprinting techniques to HIV replication complexes requires the preparation of homogeneous complexes arrested at specific positions on the template. To achieve these complexes, a technique was applied that has proved successful in halting *in vitro* transcription catalyzed by *E. coli* RNA polymerase (19). In this case, by supplying an incomplete series of NTPs, transcription was halted at a position corresponding to the missing nucleotide. Using a similar approach with HIV-1 RT, we observed continued polymerization (data not shown), which possibly reflects the infidelity of the HIV enzyme. This could be corrected by including, in a set of elongating dNTPs a chain-terminating ddNTP. The dNTP/ddNTP mixtures required to arrest polymerization at positions +1, +4, +10, and +19 on our model template·primer are illustrated in Fig. 1*a*.

High-resolution gel electrophoretic analysis of the products from polymerization reaction mixtures arrested at positions +1, +10, and +19 is shown in Fig. 1*b*. The presence of homogeneous polymerization products indicates that chain termination was highly efficient. In addition, the absence of shorter products in the complexes arrested at positions +10 and +19 is a good indication that HIV-1 RT did not pause during polymerization to give a prematurely aborted nascent DNA.

Analysis of Template DNA After Primer Extension by 1 nt. Preliminary experiments with heterodimer HIV-1 RT and the synthetic template·primer DNA indicated that a stable binary complex could not be readily achieved (W.M. and H.H., unpublished observations). Consequently, we elected to study a complex of RT with both its primer and template strands after addition of a single base to the primer (+1 complex) as reference. The results of this analysis are presented in Fig. 2*a*.

Hydroxyl radical treatment of template DNA in the absence of RT (Fig. 2*a*, lane 3) indicates that each sugar moiety is equally accessible to attack. However, after addition of a single base to the primer, wild-type p66/p51 RT protects a region of 18 bases from positions +3 to −15 (lanes 1 and 4). Rather than observing full protection, this region is interrupted by a "window" of bases between positions −8 and −11 that is accessible to hydroxyl radical cleavage (schematic representation in Fig. 3). In addition to this "window" of accessibility, a surprising observation was enhanced cleavage of template DNA upstream to the site of polymerization (position −15). The position of these enhanced cuts, relative to the polymerase catalytic center, is reminiscent of RT-associated RNase H activity, which cleaves an RNA template hybridized to a DNA primer 15–17 bases upstream of the polymerization site (20, 21). Comparative footprinting studies using a preparation of mutant p66/p51 HIV-1 RT lacking RNase H activity yet fully competent as a polymerase (15, 16) strongly suggest that this C-terminal domain of p66

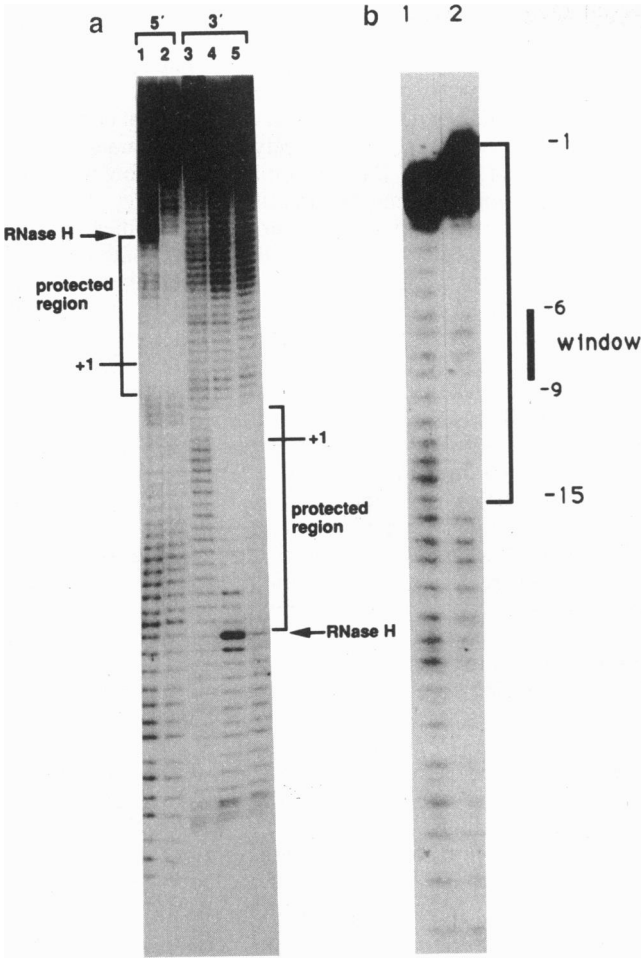

FIG. 2. (*a*) Hydroxyl radical footprinting of template DNA after arrest of RT-catalyzed DNA synthesis in the +1 register (i.e., addition of a single base to the primer). Lanes: 1 and 4, wild-type RT; 2 and 5, RNase H-deficient RT; 3, no RT; 1 and 2, 5′-^{32}P-labeled template; 4 and 5, 3′-^{32}P-labeled template. The position at which DNA synthesis is initiated has been indicated (+1). Note the region of hyperaccessibility at the 3′ extremity of the binding site (RNase H) on the template strand. (*b*) Footprint analysis of primer DNA containing polymerization complexes arrested in the +1 register (lane 2). Lane 1 shows hydroxyl radical treatment of primer DNA in the absence of RT. The region accessible to hydroxyl radicals between positions −6 and −9 (window) is indicated by a bar. Primer DNA contained the radioactive label at its 5′ terminus. Note that hyperaccessibility is not observed with primer DNA in the presence of RT.

RT is in some way responsible for the enhanced cleavage. Hypersensitivity to hydroxyl radicals was not observed in the presence of the RNase H-deficient mutant p66$^{E\rightarrow Q}$/p51, whereas the protected region itself remained unaffected (Fig. 2*a*, lanes 2 and 5). Such enhanced cleavage around position −15 might reflect increased accessibility of the template due to a local conformational change induced by the RNase H domain of template-bound RT. The alternative explanation, which we feel is less probable, is that hydroxyl radical treatment leads to DNA modification mimicking an RNA environment. Support for the former hypothesis was provided by substituting a primer·template that had been pretreated with hydroxyl radicals; under these conditions, hypersensitivity was not observed with wild-type RT (data not shown).

For the sake of clarity, footprinting experiments were performed with template DNA containing the radioactive label at either the 3′ (Fig. 2*a*, lanes 4 and 5) or 5′ (lanes 1 and 2) terminus, which yielded identical results.

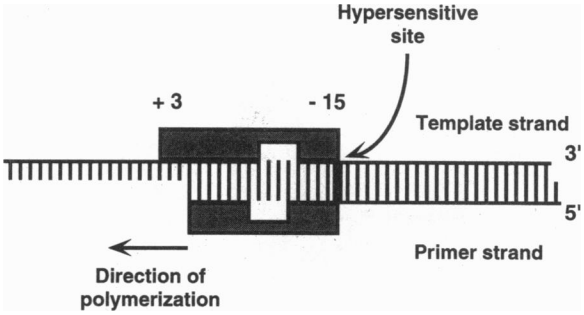

FIG. 3. Schematic representation of the hydroxyl radical footprints obtained on template and primer strands. Shaded areas indicate protection regions of the primer and template by both wild-type and RNase H-deficient p66/p51 HIV RT between positions +3 and −15. The arrow (hypersensitive site) indicates the position of enhanced hydroxyl radical cleavage due to alterations in template structure induced by the RNase H domain of p66/p51 RT.

Hydroxyl Radical Treatment of Primer DNA in a +1 Complex. The hydroxyl radical footprint of the primer strand extended by a single base (+1 complex) is illustrated in Fig. 2*b*. Analysis of this complex indicates that a region of 15 bases is protected. While not as clearly visible as observed with the template strand, an accessible "window" of 4 bases, centered around positions −8 and −9, could also be observed. The results in Fig. 2*b* and several related experiments indicate that the window is not positioned symmetrically over the template and primer strands but rather that, on the primer, the window is shifted 1 or 2 bases toward the direction of polymerization (for a diagrammatic representation, see Fig. 3). In contrast to footprint data obtained with the template strand (Fig. 2*a*), we observed no hyperreactivity of base sugars toward the 3′ end of the protected region. A similar series of footprinting studies were also performed with homodimeric p66 HIV-1 RT, which Hostomska *et al.* (22) have suggested as the precursor of the p66/p51 heterodimer. Although not shown here, the protection pattern was unaltered relative to those obtained with the heterodimer, indicating that both enzyme forms interacted similarly with their template and primer. Experiments with the p51 polypeptide indicated that DNA polymerase activity was too low to permit a footprint analysis.

Analysis of Template DNA Containing Complexes Arrested in the +4, +10, and +19 Registers. Hydroxyl radical footprinting patterns on the DNA template after translocation of wild-type p66/p51 RT into the registers +4, +10, and +19, compared with a +1 complex, are illustrated in Fig. 4. Although template sequences that interact with the enzyme vary with each register, the four footprints do not differ qualitatively, indicating (*i*) protection of 18 bases, (*ii*) the window of accessibility, and (*iii*) hyperreactivity to hydroxyl radicals upstream from the polymerase active center. Such observations would indicate that the interaction between HIV-1 RT and the template we have chosen is not base-specific. Furthermore, both the window of accessibility and position of hyperreactivity at position −15 (Fig. 2*a*) move in accordance with the registers of DNA synthesis, reflecting correct translocation.

Molecular Modeling Suggests A Conformation for the Template·Primer. The results of our hydroxyl radical footprinting studies with both the template and primer strands are represented schematically in Fig. 3, and Fig. 5 depicts an interpretation of these results using nucleic acid templates modeled in both the A and B forms. Comparison of the footprinting patterns suggests that the B form is rather unlikely. B conformation of the template when complexed with both wild-type and RNase H-deficient p66/p51 HIV-1 RT would imply that there exists a window at the interface

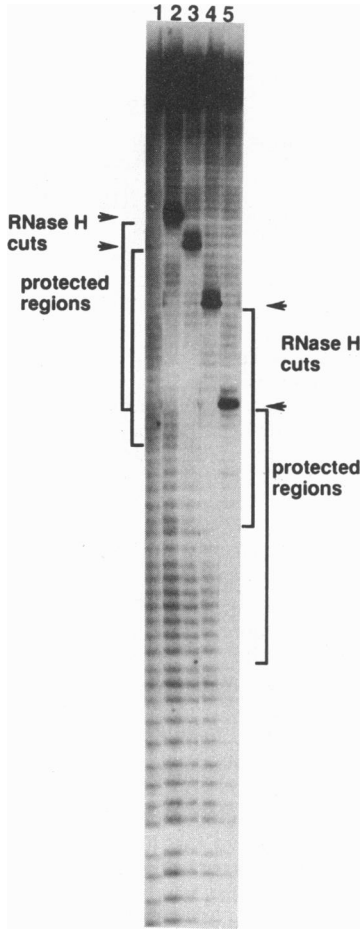

FIG. 4. Footprint analysis of template DNA containing polymerization complexes arrested in the +1 (lane 2), +4 (lane 3), +10 (lane 4), and +19 (lane 5) registers. Lane 1 shows hydroxyl radical treatment of template DNA in the absence of RT. Template DNA was labeled at its 5′ terminus. Hyperaccessible bases at the 3′ end of the polymerase binding site have been indicated for each polymerization complex (arrows). All experiments were conducted with wild-type HIV-1 RT.

between protein and nucleic acid, at which the DNA is accessible all around. The A-form model, in contrast, allows full contact of RT with one side of the DNA over 18 bases, which corresponds to ≈5.4 nm. That the accessible bases within this stretch are located at one side of the template, positioned opposite to the protein, supports this model.

DISCUSSION

Although considerable progress has recently been made in determining the structure of HIV-1 RT, either in the presence of the nonnucleoside inhibitor Nevirapine (7) or duplex DNA (6), little data exist regarding how the enzyme interacts with its RNA and DNA template·primers after initiation of DNA synthesis. While polymerization controlled by an RNA template cannot easily be followed due to its simultaneous hydrolysis by RT-associated RNase H activity (20, 21, 23), it is possible to construct systems closely mimicking viral (+)-strand synthesis (13) by use of a DNA template·primer. DNA synthesis is a dynamic process; application of hydroxyl radical footprinting requires "freezing" of polymerization at specific positions. In the present communication, we have devised a model template·primer from which controlled polymerization could be achieved by inclusion of chain-terminating ddNTPs in the reaction mixture. This has allowed us to study complexes arrested in the +1, +4, +10, and +19 registers with respect to both the template and primer strands. Analysis of these complexes indicates that an 18-nt region of template·primer (18 bases of template and 15 bases of primer) interacts with p66/p51 HIV-1 RT. Similarity of these footprinting patterns obtained with different complexes suggests that the interaction is largely sequence-independent.

Domains of HIV-1 RT participating in protecting the primer and template can be identified by using structural information obtained from crystallographic studies. Kohlstaedt *et al.* (7) created a model of the RT–template complex by placing a double-stranded nucleic acid template in the A form on their 0.35-nm structure of heterodimeric HIV-1 RT. Their model suggests that the nucleic acid template is positioned in a groove of RT, contacting one side of the protein, which is consistent with the data presented here. The model of Kohlstaedt *et al.* (7) indicates that a cleft exists in the downstream region at the polymerization site. This cleft is formed by two domains, designated finger and thumb, into which the nucleic acid template fits. On the basis of our footprinting data, we suggest that these domains wrap around the template during complex formation leading to full protection in the region between positions +3 and −7. This view is supported by the finding of Arnold *et al.* (6), who showed by a comparison of the electron densities of RT with and without template that protein mass at the polymerization site is moved during complex formation.

We suggest that protection of DNA in the upstream region between positions −12 and −15 observed in our analysis is the consequence of an interaction with the C-terminal RNase H domain of the 66-kDa polypeptide. This is plausible, since RNase H cuts the RNA template of an RNA·DNA hybrid at position −15, indicating spatial proximity of the RNase H domain and this DNA region, in accordance with the x-ray models. Such a notion would also be consistent with data obtained with the purified HIV-1 RNase H domain, which interacts with 4 bp of a synthetic RNA·DNA hybrid (30). The consistency of the footprinting and x-ray data is quite remarkable, if the A conformation of the nucleic acid template is assumed. However, there is one conflicting result that concerns the distance between the polymerase and RNase H centers of RT. Crystallographic data suggest that a stretch of 20 bases in the A conformation would fit the space between the two sites. Footprinting studies, in accordance with RNase H activity mapping studies, show that cutting occurs at position −15 or even closer to the polymerase active site (20, 21).

Our footprinting studies might provide an explanation for this discrepancy. Data presented in this communication indicate that RT-associated RNase H induces a conformational change selectively in the template strand, leading to enhanced accessibility of base sugars toward hydroxyl radicals. Accessibility of a single strand within the region protected by RT is reminiscent of footprinting data obtained with *E. coli* RNA polymerase bound at the promoter. A region of 10 bp within the promoter, encompassing the "transcription bubble," becomes accessible to hydroxyl radicals when an open complex was formed, indicative of DNA unwinding and strand separation (12, 24–26). A similar conformational change might occur at position −15 of our template·primer when the C-terminal RNase H-containing domain of p66 RT interacts with the template. The proposed alternative winding of template·primer around position −15 upon RT binding, with concomitant displacement of bases further upstream, would accommodate the distance between the polymerase and RNase H active sites determined from crystallographic studies (6, 7). Whether this speculation is correct must await high-resolution studies of cocrystals containing RT and template·primer, since the available data (6) do not allow a decision to be made from resolution at 0.7 nm.

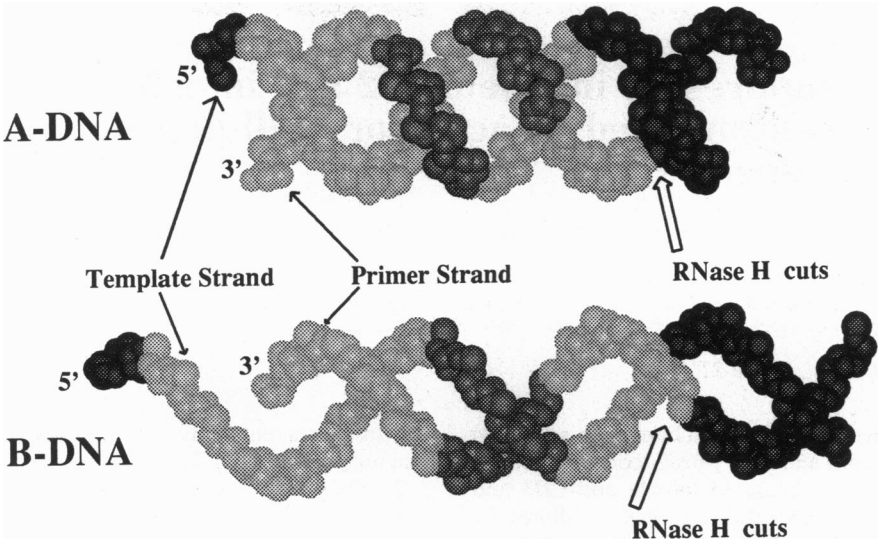

FIG. 5. Visualization of contacts between p66/p51 HIV-1 RT and template DNA using DNA models in the A and B conformations. DNA in the canonical A (*Upper*) and B (*Lower*) forms is modeled by space-filling spheres representing the sugar phosphate backbone. All hydrogen atoms, including the base side chains, are omitted. The radii of the spheres correspond to the van der Waals radii of the respective atoms. Nucleotides interacting with RT are indicated by lightly shaded spheres. Darkly shaded spheres indicate those bases in the complex whose sugar moieties are accessible, and solid spheres depict noninteracting bases. The base positions at which enhanced sensitivity to hydroxyl radicals is observed are indicated by open arrows.

Finally, although not presented in this communication, we have noted a similar mode of interaction using the 66-kDa form of HIV-1 RT. Such might not be unexpected, based on observations that homodimer p66 RT is as active as the p66/p51 form with respect to both polymerase and RNase H activity (27–29). Unfortunately, weak binding of purified p51 RT to template·primer precluded a footprint analysis with this polypeptide. However, construction of a deletion derivative of p51 that displays enhanced polymerase activity (P. Jacques, K. Howard, and S.F.J.LeG., unpublished results) should permit analysis of p51-catalyzed polymerization complexes, from which the contribution of the RNase H domain (which is absent in p51 RT) to the footprinting patterns observed here can be better assessed.

H.H. thanks Drs. P. Dennis and A. Whelan for discussion and the Bundesministerium fur Forschung und Technologie for Support (Research Grant II-108-90). S.F.J.LeG. is supported by grants from the National Institutes of Health (AI 31147 and GM 46632). The support of a North Atlantic Treaty Organization Collaborative Research Grant (CRG 900.471) to H.H. and S.F.J.LeG. is also gratefully acknowledged.

1. Larder, B. A. & Kemp, S. D. (1989) *Science* **246,** 1155–1158.
2. St. Clair, M. H., Martin, J. L., Tudor-Williams, G., Bach, M. C., Vavro, C. L., King, D. M., Kellam, P., Kemp, S. D. & Larder, B. A. (1991) *Science* **253,** 1557–1559.
3. Nunberg, J. H., Schleif, W. A., Boots, E. J., O'Brien, J. A., Quintero, J. C., Hoffmann, J. M., Emini, E. A. & Goldman, M. E. (1991) *J. Virol.* **65,** 4887–4892.
4. Richman, D., Shih, C.-K., Lowy, I., Rose, J., Prodanovich, P., Goff, S. & Griffin, J. (1991) *Proc. Natl. Acad. Sci. USA* **88,** 11241–11245.
5. Lederer, H., Schatz, O., May, R., Crespi, H., Darlix, J. L., Le Grice, S. F. J. & Heumann, H. (1992) *EMBO J.* **11,** 1131–1139.
6. Arnold, E., Jacobo-Molina, A., Nanni, R. G., Williams, R. L., Lu, X., Ding, J., Clark, A. D., Jr., Zhang, A., Ferris, A. L., Clark, P., Hizi, A. & Hughes, S. H. (1992) *Nature (London)* **357,** 85–89.
7. Kohlstaedt, L. A., Wang, J., Friedmann, J. M., Rice, P. A. & Steitz, T. A. (1992) *Science* **256,** 1783–1790.
8. Tullius, T. D. & Dombroski, B. A. (1986) *Proc. Natl. Acad. Sci. USA* **83,** 5469–5473.
9. Zorbas, H., Rogge, M., Meisterernst, M. & Winnaker, E.-L. (1989) *Nucleic Acids Res.* **17,** 7735–7743.
10. Siebenlist, U. & Gilbert, W. (1980) *Proc. Natl. Acad. Sci. USA* **77,** 122–126.
11. Dixon, W. J., Hayes, J. H., Levin, J. R., Weidner, M. F., Dombroski, B. A. & Tullius, T. D. (1991) *Methods Enzymol.* **208,** 380–413.
12. Schickor, P., Metzger, W., Werel, W., Lederer, H. & Heumann, H. (1990) *EMBO J.* **9,** 2215–2220.
13. Varmus, H. & Swanstrom, R. (1984) in *RNA Tumor Viruses,* eds. Weiss, R., Teich, N., Varmus, H. & Coffin, J. (Cold Spring Harbor Lab. Press, Plainview, NY), pp. 369–512.
14. Le Grice, S. F. J. & Grüninger-Leitch, F. (1990) *Eur. J. Biochem.* **187,** 307–314.
15. Schatz, O., Cromme, F., Grüninger-Leitch, F. & Le Grice, S. F. J. (1989) *FEBS. Lett.* **257,** 311–314.
16. Schatz, O., Cromme, F., Naas, T., Lindemann, D., Mous, J. & Le Grice, S. F. J. (1990) in *Oncogenesis and AIDS,* ed. Papas, T. (Portfolio, Houston), pp. 304–315.
17. Howard, K. J., Frank, K. B., Sim, I. S. & Le Grice, S. F. J. (1991) *J. Biol. Chem.* **266,** 23003–23009.
18. Maniatis, T., Fritsch, E. F. & Sambrook, J. (1989) *Molecular Cloning: A Laboratory Manual* (Cold Spring Harbor Lab. Press, Plainview, NY), pp. 10.59–10.61.
19. Metzger, W., Schickor, P. & Heumann, H. (1989) *EMBO J.* **8,** 2745–2754.
20. Wöhrl, B. M. & Moelling, K. (1990) *Biochemistry* **29,** 10141–10147.
21. Furfine, E. S. & Reardon, J. E. (1991) *J. Biol. Chem.* **266,** 406–412.
22. Hostomska, Z., Matthews, D. A., Davies, J. F., II, Nodes, B. F. & Hostomsky, Z. (1991) *J. Biol. Chem.* **266,** 14697–14702.
23. Schatz, O., Mous, J. & Le Grice, S. F. J. (1990) *EMBO J.* **9,** 1171–1176.
24. Kirkegaard, K., Buc, H., Spassky, A. & Wang, J. C. (1983) *Proc. Natl. Acad. Sci. USA* **80,** 2544–2548.
25. Siebenlist, U., Simpson, R. B. & Gilbert, W. (1980) *Cell* **20,** 269–281.
26. von Hippel, P. H., Baer, D. G., Winter, R. B. & Berg, O. G. (1982) in *Promoter Structure and Function,* eds. Rodriguez, R. L. & Chamberlin, M. J. (Praeger, New York), pp. 3–31.
27. Restle, T., Müller, B. & Goody, R. S. (1990) *J. Biol. Chem.* **265,** 8986–8988.
28. Müller, B., Restle, T., Kuhnel, H. & Goody, R. S. (1991) *J. Biol. Chem.* **266,** 14709–14713.
29. Restle, T., Müller, B. & Goody, R. S. (1992) *FEBS Lett.* **300,** 97–100.
30. Cirino, N. M., Kalayjian, R. C., Jentoft, J. & Le Grice, S. F. J. (1993) *J. Biol. Chem.*, in press.